Zebrafish with Mutations in Mismatch Repair Genes Develop Neurofibromas and Other Tumors

Harma Feitsma,[1] Raoul V. Kuiper,[2] Jeroen Korving,[1] Isaac J. Nijman,[1] and Edwin Cuppen[1]

[1]Hubrecht Institute for Developmental Biology and Stem Cell Research, Cancer Genomics Center and [2]Faculty of Veterinary Medicine, Department of Pathobiology, Utrecht University, Utrecht, the Netherlands

Abstract

Defective mismatch repair (MMR) in humans causes hereditary nonpolyposis colorectal cancer. This genetic predisposition to colon cancer is linked to heterozygous familial mutations, and loss-of-heterozygosity is necessary for tumor development. In contrast, the rare cases with biallelic MMR mutations are juvenile patients with brain tumors, skin neurofibromas, and café-au-lait spots, resembling the neurofibromatosis syndrome. Many of them also display lymphomas and leukemias, which phenotypically resembles the frequent lymphoma development in mouse MMR knockouts. Here, we describe the identification and characterization of novel knockout mutants of the three major MMR genes, *mlh1, msh2*, and *msh6*, in zebrafish and show that they develop tumors at low frequencies. Predominantly, neurofibromas/malignant peripheral nerve sheath tumors were observed; however, a range of other tumor types was also observed. Our findings indicate that zebrafish mimic distinct features of the human disease and are complementary to mouse models. [Cancer Res 2008;68(13):5059–66]

Introduction

Mismatch repair (MMR) corrects small replication errors that are caused by the DNA polymerase and skipped by its proofreading capacity (1). In humans, defective MMR is associated with early-onset colorectal cancer in the hereditary nonpolyposis colorectal cancer (HNPCC) syndrome (2). According to the second-hit hypothesis (3), only one extra mutation, one that inactivates the wild-type allele of the MMR gene, is necessary to create a genomic instable environment that strongly enhances cancer development. Perhaps due to the high cell turnover in the colon, this organ is most prone to the loss-of-heterozygosity followed by tumorigenesis, but several other types of tumors have also been found in HNPCC patients (4).

In the years following the discovery of HNPCC, continuous monitoring of HNPCC families has revealed several cases of humans with innate inactivating mutations in both alleles of a MMR gene, resulting from inbreeding or coincidence (5–19). These patients lack the MMR protein from the beginning and therefore develop cancer at extremely early ages, generally before the age of 10 years. From a summary of the tumors that occurred in this group of patients (Table 1), it becomes clear that the tumor spectrum is markedly different from HNPCC patients. Most striking is the high frequency of brain tumors, such as glioblastoma, medulloblastoma, oligodendroglioma, primitive neuroectodermal tumor (PNET), and astrocytoma. In combination with a high incidence of neurofibromas in the skin and café-au-lait spots, this resembles the neurofibromatosis type I syndrome (20). Second most frequent are lymphomas and leukemias (Table 1). Gastrointestinal tumors occur (Table 1) but at much lower rate than in HNPCC patients and at a later age than the other tumor types. Apparently, constant genomic instability in all cells causes different cancers, which prompted some authors to call this the MMR deficiency syndrome (13) or childhood cancer syndrome (19), whereas others consider it a variant of Turcot's syndrome (14, 15, 21). A number of cases were found for the four most important MMR genes, *MSH2, MLH1, MSH6*, and *PMS2*. Striking is that biallelic inactivation of PMS2 leads to juvenile cancer, whereas heterozygous mutated PMS2 has not frequently been detected in cases of HNPCC (2).

To obtain animal models for HNPCC, mouse knockouts for all MMR genes have been generated (22–33). Homozygous mutants predominantly die of lymphomas (Table 1). Intestinal tumors occur at much lower frequencies than in HNPCC, which led some researchers to conclude that these mouse mutants were not properly modeling HNPCC. However, when comparing the tumor spectra of these homozygous mouse models to the spectrum of humans with biallelic mutations (Table 1), it becomes clear that they are similar in terms of frequent lymphoma development and relatively low abundance of gastrointestinal tumors. A difference is that brain tumors are very rare and neurofibromas and café-au-lait spots are absent in mouse MMR knockouts (Table 1).

Here, we describe the isolation of zebrafish mutants for the MMR genes *mlh1, msh2*, and *msh6* and show that homozygous mutants of all three lines develop neoplasms, with a frequency of 6% to 45%. Most frequently, neurofibromas/malignant peripheral nerve sheath tumors (MPNST) in the eye and abdomen were observed; however, other tumor types also occurred, such as PNET in the brain and hemangiosarcoma on the head.

Materials and Methods

PCR. The sequences of all oligonucleotides that were used are given in Supplementary Table S1.

Generation of mutant zebrafish lines. All animal experiments were approved by the Animal Care Committee of the Royal Dutch Academy of Science according to the Dutch legal ethical guidelines. For obtaining *msh6* and *msh2* mutant fish amplicons that covered most of the large exon 4 of the zebrafish *msh6* gene and exon 5 and 6 of the zebrafish *msh2* gene, respectively, were used in an ethylnitrosourea (ENU)–driven target-selected mutagenesis screen (34). The obtained mutant fish were outcrossed with wild-type fish, and heterozygous offspring was subsequently incrossed. Genotyping was done either by PCR amplification and resequencing or by using KASPAR genotyping technology (Kbioscience). The *mlh1 (hu1919)* mutants were generated as described previously (35).

Note: Supplementary data for this article are available at Cancer Research Online (http://cancerres.aacrjournals.org/).

Requests for reprints: Edwin Cuppen, Hubrecht Institute for Developmental Biology and Stem Cell Research, Uppsalalaan 8, 3584 CT Utrecht, the Netherlands. Phone: 31-30-2121969; Fax: 31-30-2516554; E-mail: e.cuppen@niob.knaw.nl.

doi:10.1158/0008-5472.CAN-08-0019

Table 1. Tumors in human patients with biallelic inactivation of MMR genes

Gene	*n*	Cancer (%)	Brain tumor*	Lymphoma	Leukemia	GI tumor	Skin tumor	Other	CALS	References
Human										
MSH2	3		1	1	1				1	(5, 6)
MLH1	11		4	2	2	2	4 †	2	10	(7–11)
MSH6	10		8	4	1	4			9	(10–14)
PMS2	27		17	5	4	10		3	20	(11, 15–19)
Total (%)	51		30 (59)	12 (24)	8 (16)	16 (31)	4 (8)	5 (10)	40 (78)	
Mouse										
Msh2	207	204 (99)	4	161	10	60	12	18		(22–26)
Mlh1	76	69 (91)		41		40	8			(27–29)
Msh6	35	35 (100)		20	2	8	7	8		(30–32)
Pms2	45	34 (76)		31				6		(28, 29, 33)
Total (%)	363	342 (94)	4 (1) ‡	253 (74) ‡	12 (4) ‡	108 (32) ‡	27 (8) ‡	32 (9) ‡		

Abbreviations: GI, gastrointestinal; CALS, cafe-au-lait spots.
*In humans: glioma, glioblastoma, medulloblastoma, oligodendroglioma, PNET, supratentorial PNET, and astrocytoma; in mouse: not further specified.
† Neurofibromas.
‡ Percentage of mice with this type of tumor of the total number of mice that developed cancer.

Reverse transcription-PCR and quantitative PCR. RNA was isolated from tail tissue of adult zebrafish and wild-type embryos using FastRNA Pro Green kit (Q-biogene) and reverse transcribed by using the RETROscript kit (Ambion). For *msh2* reverse transcription-PCR (RT-PCR), cDNA-specific primers on the boundary of exons 3 and 4 and within exon 6 were used, resulting in a 354-bp fragment in the wild-type. For *msh6* quantitative PCR, cDNA-specific primers within exon 6 and within exon 8 were used. As a control, the *msh2* primers mentioned above were used. The reactions contained iQ SYBR Green Supermix (Bio-Rad) and were run and analyzed with the MyIQ single color real-time PCR detection system and software (Bio-Rad). A dilution series of wild-type cDNA was used as a standard. All genotypes were run in 5-fold. The cDNA concentrations were calculated in arbitrary units compared with the wild-type average and expressed as the ratio of msh6 to msh2.

Microsatellite instability. Two mononucleotide (A_{22} and A_{25}) and two dinucleotide markers (CA_{17} and CA_{22}) were PCR amplified using embryonic DNA as a template by using one fluorescently labeled and one unlabeled primer per marker. The appropriate volume of PCR product was mixed with 0.5 μL GeneScan 500 LIZ size standard (Applied Biosystems) in 5 μL mQ, denatured for 5 min at 95°C and subsequently run on an ABI3730XL capillary DNA analyzer (Applied Biosystems). Product lengths were analyzed using Genemapper software (Applied Biosystems).

Cancer development. Homozygous mutant fish and heterozygous siblings of all three mutant lines were monitored weekly. Animals with signs of disease or apparent cell masses were sacrificed. Fish were fixed in 4% paraformaldehyde at 4°C for 4 d, decalcified in 0.25 mol/L EDTA (pH 8) at room temperature for 2 d, and embedded in paraffin. Six-micrometer sections were taken at different positions of the body and were stained with H&E for histologic characterization. All surviving fish were sacrificed at 24 mo of age and were analyzed similarly. Tumor incidences were analyzed statistically using one-tailed Fisher's exact tests.

Results

Generation of MMR mutants in zebrafish. Using ENU-driven target-selected mutagenesis, we isolated three zebrafish mutants with putative loss-of-function mutations in the major MMR genes *msh6, msh2*, and *mlh1*.

The *msh6* mutant (*hu1811*) carries a point mutation causing a premature stop codon in the large fourth exon (Fig. 1*A*). This exon is well conserved in comparison with the similarly large fourth exon of the human *MSH6* gene. According to the database of the International Society for Gastrointestinal Tumors,[3] among HNPCC families, there are several alleles known of point mutations causing premature translation termination in this exon, increasing the likelihood that our zebrafish mutation will be pathogenic. We could not confirm the knockout phenotype at the protein level in the zebrafish mutant, as we were not able to find an anti-MSH6 antibody that recognizes the zebrafish protein. However, we could show by quantitative PCR that the levels of *msh6* transcript are decreased to ~44% of the wild-type level in heterozygous and ~15% in homozygous mutants, presumably due to nonsense-mediated decay of the premature stop codon–containing transcript (Fig. 1*B*).

The mutation in *msh2* (*hu1886*) changes the G of the splice donor site of exon 5 to an A (Fig. 1*A*). Using RT-PCR, we could show that it results in a 150 bp shorter mRNA (Fig. 1*C*). Sequencing of this product showed that this is the result of an in-frame deletion of exon 5 (Fig. 1*C*). The genomic organization of the *msh2* gene is highly homologous from human to fish, including complete conservation of the exon-intron boundaries of exon 5 (Supplementary Fig. S1). Interestingly, in humans, in-frame deletion of exon 5 of *MSH2* is the most common mutation in HNPCC families, accounting for 11% of all known pathogenic *MSH2* mutations (36). It results in an incomplete protein (37), and carriers have a high risk of developing cancers (38), which generally are microsatellite instable (39). This suggests that the splice site mutation of *msh2* in zebrafish results in loss of function of the gene and provides a translational animal model for *MSH2*-driven disease in humans.

The third MMR mutant that is used in this study contains a premature stop mutation in *mlh1* (*hu1919*; Fig. 1*A* and *D*). We recently showed that this mutation results in full loss-of-function of MLH1 and causes a strong meiotic phenotype (35).

MMR-deficient zebrafish show microsatellite instability. One of the hallmarks of defective MMR is instability of microsatellite sequences (2). We studied microsatellite instability (MSI) within two mononucleotide and two dinucleotide repeat loci in the germ

[3] http://www.insight-group.org

line of *msh2* and *msh6* mutants—*mlh1* mutant males are sterile (35) and could therefore not be included in this assay. Homozygous mutant males were crossed with wild-type females and microsatellites were typed in the progeny. As the latter are heterozygous and thus MMR proficient, any observed clonal instability should have occurred in the germ line of the male founder (Fig. 2). Three percent of offspring of $msh2^{-/-}$ males have altered microsatellite lengths, both in mononucleotide and dinucleotide repeat sequences. $Msh6^{-/-}$ progeny predominantly shows instability of mononucleotide markers in 4% of the cases. No MSI was detected in progeny from wild-type or heterozygous males (Table 2).

MMR-deficient zebrafish develop tumors. From age 6 months, MMR mutant zebrafish started developing cancer. Tumors were only found in homozygous mutants and mostly developed in the 2nd year of life (Table 3). The cancer incidence was relatively low but was much higher than generally found in wild-types, 33% on average for all three lines together. In total, 25 tumors were detected, of which 13 in $mlh1^{-/-}$, 11 in $msh6^{-/-}$, and 1 in $msh2^{-/-}$ fish (Table 3).

The tumor frequency in homozygous mutants was significantly higher than in heterozygous siblings for the *mlh1* (n = 29 for homozygotes, n = 30 for heterozygotes; $P = 2 \times 10^{-5}$) and *msh6* (n = 31 for homozygotes, n = 12 for heterozygotes; P = 0.01) mutants. This is not the case for the *msh2* mutant (n = 16 for homozygotes, n = 15 for heterozygotes; P = 0.5), as the number of animals and tumors is low. This is most likely caused by the reduced general fitness of the line. For all three mutants together, the difference in tumor frequency is highly significant (n = 76 for homozygotes, n = 57 for heterozygotes; $P = 1 \times 10^{-7}$).

Tumors are characterized as neurofibromas/MPNST and other types. Frequently, tumors were poorly differentiated; however, a high proportion (76%) showed features consistent with piscine neural crest origin tumors, such as unencapsulated growth of spindle-shaped neoplastic cells in interconnected fascicles and scattered presence of pigmentary cells (iridophores and melanocytes). The neoplastic growth invaded surrounding structures, including bone and cartilage of the skull, connective tissue and sclera, and striated muscle. As clearly distinct Antoni A and B patterns were not recognized, palisading was generally absent, and whorls of tumor cells resembling Pacinian-like corpuscles were more frequently observed, the diagnosis neurofibrosarcoma was favored to malignant Schwannoma for these tumors. However, due to the lack of reliable immunohistochemical markers for these lesions in zebrafish, the distinction between these two types of MPNSTs cannot be made definitely, so that we use both characterizations together. Neurofibromas/MPNSTs were most frequent in the eye (Fig. 3*A*) and in the abdomen (not shown). Most tumors in the trunk and one extraocular cranial tumor were located dorsally, extending into the renal tissue and skeletal muscle surrounding the skull and vertebral column, or invading bones and

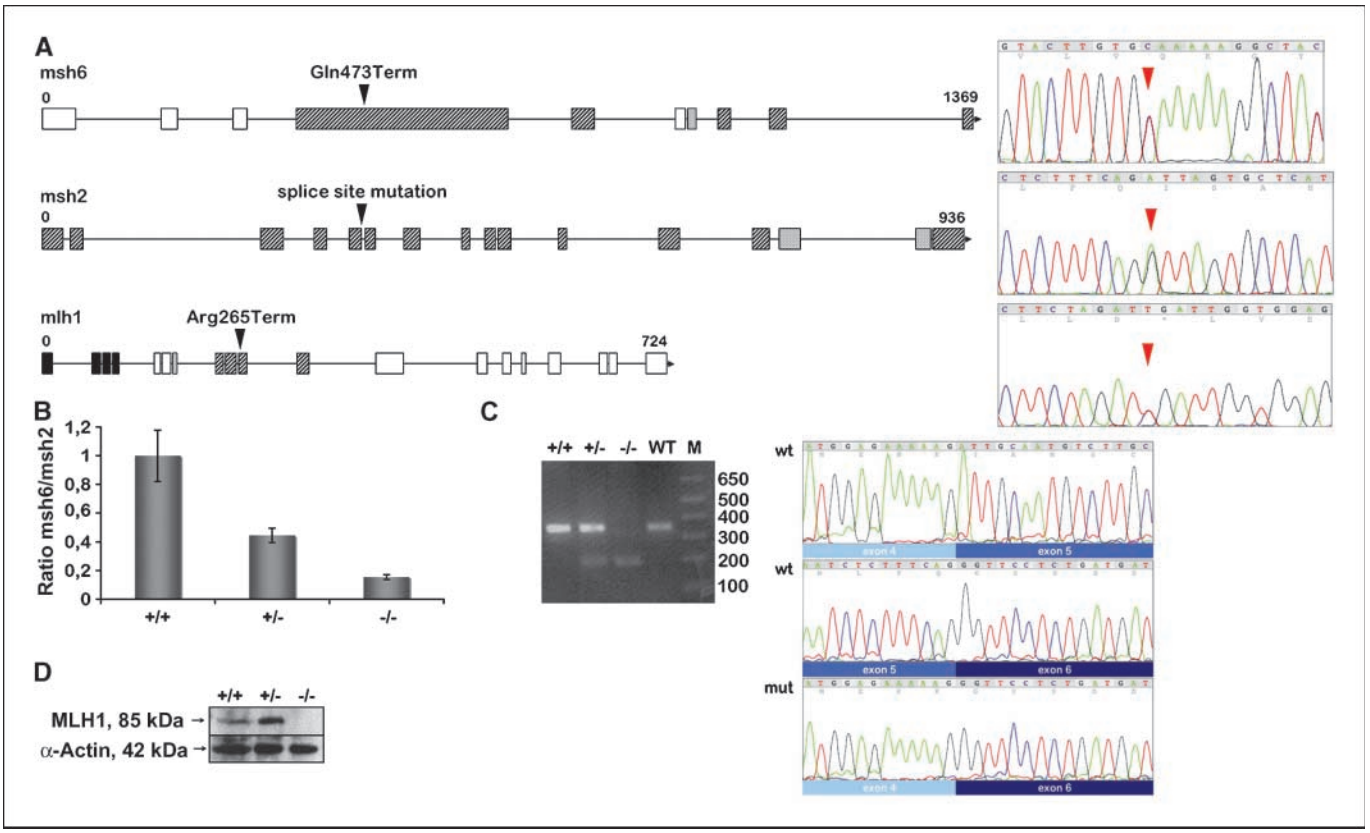

Figure 1. Molecular characterization of zebrafish mutants of three MMR genes. *A, left,* schematic overview of the gene structure and position of the point mutation. Important domains are marked: DNA MMR domains are striped; ATP/GTP binding sites are grey; ATP-binding ATPase domains are black. *Right,* sequence trace of the point mutation in the founder fish. *B,* quantitative PCR shows that the *msh6* transcript is decreased to 44% of the wild-type level in heterozygous mutants and to 15% in homozygous mutants. Ratios of *msh6* cDNA over *msh2* cDNA as a control are shown, normalized to the levels in wild-types. The differences between the genotypes are significant ($P < 0.05$). *C, left,* RT-PCR shows that the *msh2* transcript is 150 bp shorter in homozygous mutants and also partly in heterozygotes. *Right,* sequencing of the transcript reveals an in-frame deletion of exon 5 in the mutants. *Light blue*, exon 4; *blue*, exon 5; *dark blue*, exon 6. *D,* Western blot shows loss of MLH1 protein in homozygous mutants (adapted from ref. 35).

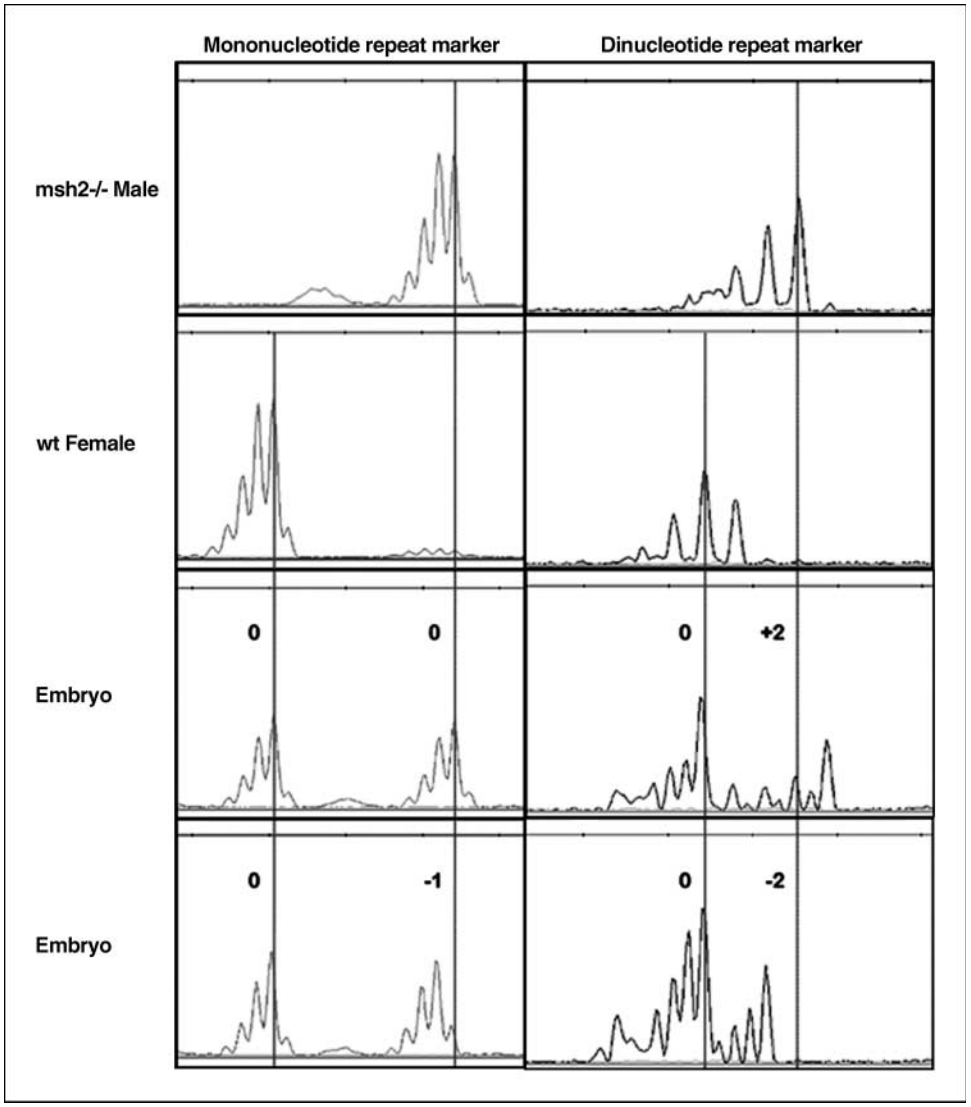

Figure 2. MSI in MMR mutant zebrafish. Examples of instability in a mononucleotide (*left*) and a dinucleotide (*right*) marker are shown. *Top row,* allele lengths of a *msh2*$^{-/-}$ male; *second row,* allele lengths of a wild-type female. Embryos of a cross of those two show changes in the paternal allele length, as shown in the two bottom rows.

cartilage of the skull. Therefore, a meningothelial component cannot be excluded, which could explain the histologic similarity between intraocular, cranial, and abdominally located neoplasms.

Furthermore, two distinct cases of cranial neural crest tumors were observed. In one case, a mass protruding from the rostral aspect of the cranium and invasively growing between the eyes histologically consisted of clusters and nests of small polygonal to cuboid cells. These cells frequently had apical cilia and were forming rosettes and tubules, separated by areas where cells were more stellate with abundant myxoid intercellular material (Fig. 3*B*). Based on the histologic appearance and localization, this tumor was diagnosed as olfactory neuroblastoma. A third type of neural

Table 2. MSI in MMR mutant zebrafish

Genotype male	Mononucleotide			Dinucleotide		
	A22	A25	Frequency (%)*	CA17	CA22	Frequency (%)*
msh2+/−	0/95	0/95	0	0/95	0/95	0
msh2−/−	4/244	9/273	3	2/272	12/272	3
msh6+/−	0/42	0/42	0	0/42	0/42	0
msh6−/−	5/219	14/222	4	0/221	1/223	0
Wild-type	0/156	0/151	0	0/147	0/154	0

*Average percentage of embryos that is instable for this type of markers.

Table 3. Tumor development in MMR mutant zebrafish

Genotype	*n*	Cancer (%)	Av. age cancer (mo)	Ocular nf.	Abdominal nf.	Other nf.	Other neural*	Cranial nonneural †
mlh1−/−	29	13 (45)	14	1	8	1	2	1
mlh1+/−	30	0 (0)						
msh2−/−	16	1 (6)	22	1				
msh2+/−	15	0 (0)						
msh6−/−	31	11 (35)	20	2	5	1		3
msh6+/−	12	0 (0)						
Total−/− (%)	76	25 (33)	17	4 (16) ‡	13 (52) ‡	2 (8) ‡	2 (8) ‡	4 (16) ‡
Total+/− (%)	57	0 (0)						

Abbreviation: nf., neurofibroma.
*Primitive neuroectodermal tumor and olfactory neuroblastoma.
† Hemangioma, hemangiosarcoma, thyroid carcinoma, and squamous cell carcinoma.
‡ Percentage of zebrafish with this type of tumor of the total number of fish that developed cancer.

crest tumor was found inside the cranium of one fish, extending from the brain through cartilage and bones of the skull into the surrounding tissues, including the eye. Histologically, the neoplasm consisted of poorly differentiated small polymorphic cells with limited amounts of basophilic cytoplasm and distinct cellular borders, growing in solid sheets (Fig. 3*C*). This morphology was consistent with PNET diagnosis.

Tumors other than those of neurectodermal of origin included a cavernous hemangioma (not shown) and a hemangiosarcoma (Fig. 3*D*), both in the head. Histologically, these lesions were characterized by plump fusiform cells growing in a cribriform pattern, with intercellular spaces frequently containing erythrocytes. Hyperplastic epithelial lesions with formation of irregular dermal islets of dysplastic epithelial cells without connection to the epidermis were observed in the head of one fish, consistent with squamous cell carcinoma (not shown). One animal showed a poorly differentiated densely cellular neoplasm located ventrally between the branchial arches, invading the tissues surrounding the ventral aorta, consisting of small cuboidal to polygonal cells with indistinct borders growing in solid sheets, with occasional palisading of tumor cells and rare formation of rosettes or follicles containing small amounts of brightly eosinophilic material. Consistent with the location of the teleost thyroid, this tumor was diagnosed as a solid thyroid carcinoma (not shown).

Although the above neoplasms showed marked invasion of the surrounding tissue, mitotic figures were infrequent in all tumors and no indications for metastasis were observed. The tumor classification was done solely on morphologic characteristics, because the necessary immunohistochemical stainings (for glial fibrillary acidic protein, synaptophysin, epithelial membrane antigen, neuronal nuclei, and s100) to confirm these tumor types did not work on zebrafish. Some exemplary tumors ($n = 5$) were stained with Ziehl-Neelsen to exclude that cell masses were the result of infections, and all were indeed negative (results not shown).

Discussion

We generated the first MMR-deficient models in zebrafish by knocking out the major MMR genes *mlh1, msh2*, and *msh6*, respectively. Homozygous mutants for *msh2* and *msh6* show MSI, which is a hallmark of defective MMR. The frequency at which we find instability (3–4%) is lower than generally observed in mice (15–40%; refs. 22, 29, 33, 40); however, this can be explained by the fact that we studied markers in the germ line, where mutations rates are usually lower than in somatic cells that were used in the mouse studies. The per generation mutation rate for a large set of repeat markers in wild-type zebrafish was found to be 1.5×10^{-4} (41), which means that it is increased around 200-fold in our mutants. In mouse somatic cells, the microsatellite mutation frequency was on average 50-fold higher in the mutant than in wild-types (40), which is a comparable increase. The observed MSI in both mononucleotide and dinucleotide repeats in *msh2* mutants and in mononucleotide repeats only in *msh6* mutants is consistent with the respective functions of MSH2 and MSH6 in repair of different types of mutations (1), although dinucleotide repeat instability has been observed in tumors of mouse *msh6* knockouts (32). Homozygous mutants of all three fish lines are prone to tumor development at low but significant incidence and primarily develop neurofibromas/MPNSTs in the eye and abdomen, but also a PNET, an olfactory neuroblastoma, a hemangioma and hemangiosarcoma, a squamous cell carcinoma, and a thyroid carcinoma were observed. Although the number of tumors is low, these data suggest that the zebrafish model resembles an important part of the phenotype of human patients, where biallelic MMR inactivation causes a neurofibromatosis type I–like phenotype, a phenotype that is not seen in mouse MMR knockouts. Similar to mouse mutants, tumors were only found in homozygous mutant fish.

Because lack of MMR results in a specific form of genomic instability in repeat sequences, we tested the hypothesis that the observed differences in tumor types in different species may be caused by the species-specific presence of repeat sequences in the coding sequence of selected tumor suppressor genes. We performed an *in silico* analysis of human genes involved in neural, gastrointestinal, or hematologic cancers or generally in many types of cancers and their mouse and zebrafish homologues, but found no significant differences in numbers of repeats between the three species (Supplementary Text, Supplementary Table S2, and Supplementary Figs. S2 and S3). Even more, targeted analysis of *neurofibromatosis I*, a strong candidate gene for neural tumors, did

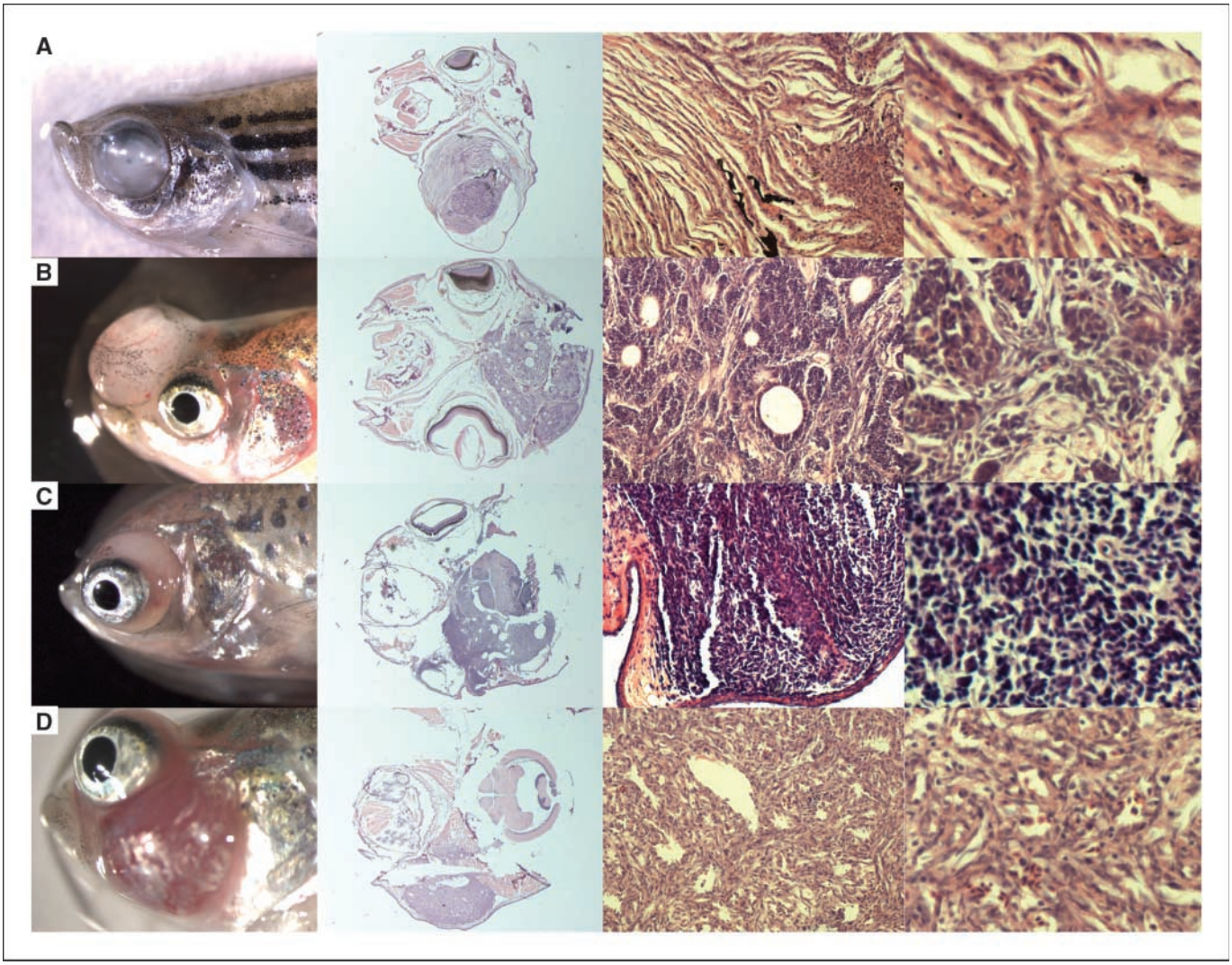

Figure 3. Tumor development in MMR mutant zebrafish. *First column,* whole mount; *second column,* cross section; *third* and *fourth columns,* higher magnifications. *A,* 18-month-old *msh6*$^{-/-}$ fish with an ocular neurofibroma. *B,* 8-month-old *mlh1*$^{-/-}$ fish with an olfactory neuroblastoma. *C,* 6-month-old *mlh1*$^{-/-}$ fish with a primitive neuroectodermal tumor in the brain. *D,* 17-month-old *msh6*$^{-/-}$ fish with a hemangiosarcoma.

not show a correlation between the number of repeat stretches and the development of neural tumors in human, mouse, and zebrafish. Nonetheless, it could still be interesting to sequence the genes containing large repeats in tumor samples of different species, to obtain information about their inactivation rates, although the presence of frameshift mutations does not necessarily mean that inactivation of the gene was essential for tumor development. Importantly, types of mutations are known to depend on selection pressure in tumor development and are thus hard to predict. A good example of this was given by Smits and colleagues, who showed that, in *msh2*-deficient background, *apc* mutations in intestinal tumors were mostly located in small dinucleotide repeats in mice wild-type in *apc*, where both alleles needed inactivation. In contrast, they were point mutations more upstream in the gene in *apc* heterozygous mice, where loss of heterozygosity had to take place (25). Here, it is therefore more likely that the organism-specific tumor spectra are the result of physiologic and anatomic differences, such as relative organ sizes and life span.

Only very recently, zebrafish has become a model for studying genetics and molecular biology of cancer. Three tumor suppressor mutants in zebrafish have been generated by reverse genetics: *tp53, pten*, and *apc* (42–44), all of which spontaneously develop tumors. Homozygous *tp53* mutants develop MPNSTs in the eye and abdomen (42), similar to the MMR mutant fish. This type of tumors was also frequent in tumor suppressor mutants from forward genetic screens, e.g., ribosomal protein mutants from a retroviral insertion screen and mutants from a screen for genome instability (45, 46). MPNSTs have been reported in several fish species, but these are certainly not the only type of neoplasm in fish. For example, *tp53* knockout medaka develop a broader range of tumors (47). Also, the ocular tumors that were found in *pten* knockout fish seem of a different type, although they have not been characterized in detail (43), and *apc* mutant fish develop intestinal and liver neoplasms (44). This, as well as the occurrence of other tumors besides neurofibromas in the MMR mutants, indicates that different genetic predispositions lead to different types of cancer, similar to the situation in humans.

Loss of MMR results in high and intermediate frequencies of hematologic defects in mice and humans, respectively. Lymphomas and leukemias generally arise due to genomic rearrangements that

result in misexpression of certain oncogenes (48). The number of known tumor suppressor genes is low, decreasing the chance that MSI will be causal to lymphoma development. The high occurrence of misrecombination in immune cells is likely the result of the large number of immunoglobin gene rearrangements that have to be made during VDJ junction and class switch recombination to create a functional immune system. Because the MMR genes *mlh1, msh2*, and *msh6* are known to play a role in class switch recombination (49–52), it is tempting to speculate that their deficiency can directly lead to immune malignancies, without the need for creating a genomic instable situation that mutates other tumor suppressors. The fact that some patients with biallelic MMR inactivation were reported to be IgA-deficient supports this idea (11). Also, MMR-deficient mice show a reduction in isotype switching (49, 50, 52). Zebrafish have three classes of immunoglobulin heavy chains, which are genomically organized by VDJ junction or alternative splicing. Class switch recombination does not occur (53), which may explain why MMR deficiency does not lead to lymphoma development in zebrafish, although lymphomas and leukemias have been observed in zebrafish (e.g., ref. 54).

The question why mice are more prone to lymphoma development than humans remains unanswered.

From our *msh2* line, we did not observe many fish dying from cancer. This is partly because homozygous mutants generally had a weak appearance and died of cancer-unrelated causes (results not shown). In addition, nearly all homozygous mutants were males and had significantly lower body weights than siblings. Although we cannot exclude that these phenotypes result from background mutations, it is striking that in humans, very few homozygous *msh2* cases were encountered whereas heterozygous patients are common, which could suggest that homozygous *msh2* inactivation reduces viability in general. It should be mentioned that such mechanism or phenotype has not been reported for *msh2* knockout mice.

Taken together, we have shown that mutants for MMR genes in zebrafish display MSI and are at increased risk for tumor development. This is similar to mice and humans, although the tumor spectra are different. From this and other recent publications, it can be concluded that zebrafish proves to be a useful cancer model that provides new insights and experimental possibilities, and complements studies in mouse and human.

Disclosure of Potential Conflicts of Interest

No potential conflicts of interest were disclosed.

Acknowledgments

Received 1/3/2008; revised 3/21/2008; accepted 4/10/2008.

Grant support: Cancer Genomics Center (Nationaal Regie Orgaan Genomics) and the European Union-funded FP6 Integrated Project ZF-MODELS.

The costs of publication of this article were defrayed in part by the payment of page charges. This article must therefore be hereby marked *advertisement* in accordance with 18 U.S.C. Section 1734 solely to indicate this fact.

We thank E. de Bruijn for help in obtaining mutant fish; M. Verheul and J. van der Belt for technical assistance; S. Linsen for initial bioinformatics help; W.G.M. Spliet, G. Grinwis, and C. Ceol for helpful discussions on tumor histology; R. van Boxtel for critically reading the manuscript; and the Wellcome Trust Sanger Center *Danio rerio* Sequencing Project for genomic sequence information.

References

1. Jiricny J. The multifaceted mismatch-repair system. Nat Rev Mol Cell Biol 2006;7:335–46.
2. Chung DC, Rustgi AK. The hereditary nonpolyposis colorectal cancer syndrome: genetics and clinical implications. Ann Intern Med 2003;138:560–70.
3. Knudson AG. Hereditary cancer: two hits revisited. J Cancer Res Clin Oncol 1996;122:135–40.
4. Lynch HT, Smyrk T. Hereditary nonpolyposis colorectal cancer (Lynch syndrome). An updated review. Cancer 1996;78:1149–67.
5. Bougeard G, Charbonnier F, Moerman A, et al. Early onset brain tumor and lymphoma in MSH2-deficient children. Am J Hum Genet 2003;72:213–6.
6. Whiteside D, McLeod R, Graham G, et al. A homozygous germ-line mutation in the human MSH2 gene predisposes to hematological malignancy and multiple cafe-au-lait spots. Cancer Res 2002;62:359–62.
7. Wang Q, Lasset C, Desseigne F, et al. Neurofibromatosis and early onset of cancers in hMLH1-deficient children. Cancer Res 1999;59:294–7.
8. Ricciardone MD, Ozcelik T, Cevher B, et al. Human MLH1 deficiency predisposes to hematological malignancy and neurofibromatosis type 1. Cancer Res 1999;59:290–3.
9. Vilkki S, Tsao JL, Loukola A, et al. Extensive somatic microsatellite mutations in normal human tissue. Cancer Res 2001;61:4541–4.
10. Poley JW, Wagner A, Hoogmans MM, et al. Biallelic germline mutations of mismatch-repair genes: a possible cause for multiple pediatric malignancies. Cancer 2007;109:2349–56.
11. Ostergaard JR, Sunde L, Okkels H. Neurofibromatosis von Recklinghausen type I phenotype and early onset of cancers in siblings compound heterozygous for mutations in MSH6. Am J Med Genet A 2005;139:96–105; discussion 96.
12. Menko FH, Kaspers GL, Meijer GA, Claes K, van Hagen JM, Gille JJ. A homozygous MSH6 mutation in a child with cafe-au-lait spots, oligodendroglioma and rectal cancer. Fam Cancer 2004;3:123–7.
13. Scott RH, Mansour S, Pritchard-Jones K, Kumar D, MacSweeney F, Rahman N. Medulloblastoma, acute myelocytic leukemia and colonic carcinomas in a child with biallelic MSH6 mutations. Nat Clin Pract Oncol 2007;4:130–4.
14. Hegde MR, Chong B, Blazo ME, et al. A homozygous mutation in MSH6 causes Turcot syndrome. Clin Cancer Res 2005;11:4689–93.
15. Hamilton SR, Liu B, Parsons RE, et al. The molecular basis of Turcot's syndrome. N Engl J Med 1995;332:839–47.
16. De Vos M, Hayward BE, Picton S, Sheridan E, Bonthron DT. Novel PMS2 pseudogenes can conceal recessive mutations causing a distinctive childhood cancer syndrome. Am J Hum Genet 2004;74:954–64.
17. De Rosa M, Fasano C, Panariello L, et al. Evidence for a recessive inheritance of Turcot's syndrome caused by compound heterozygous mutations within the PMS2 gene. Oncogene 2000;19:1719–23.
18. De Vos M, Hayward BE, Charlton R, et al. PMS2 mutations in childhood cancer. J Natl Cancer Inst 2006; 98:358–61.
19. Kruger S, Kinzel M, Walldorf C, et al. Homozygous PMS2 germline mutations in two families with early-onset haematological malignancy, brain tumours, HNPCC-associated tumours, and signs of neurofibromatosis type 1. Eur J Hum Genet 2008;16:62–72.
20. Ferner RE. Neurofibromatosis 1 and neurofibromatosis 2: a twenty first century perspective. Lancet Neurol 2007;6:340–51.
21. Leung SY, Chan TL, Chung LP, et al. Microsatellite instability and mutation of DNA mismatch repair genes in gliomas. Am J Pathol 1998;153:1181–8.
22. de Wind N, Dekker M, Berns A, Radman M, te Riele H. Inactivation of the mouse Msh2 gene results in mismatch repair deficiency, methylation tolerance, hyperrecombination, and predisposition to cancer. Cell 1995;82:321–30.
23. Reitmair AH, Redston M, Cai JC, et al. Spontaneous intestinal carcinomas and skin neoplasms in Msh2-deficient mice. Cancer Res 1996;56:3842–9.
24. Reitmair AH, Schmits R, Ewel A, et al. MSH2 deficient mice are viable and susceptible to lymphoid tumours. Nat Genet 1995;11:64–70.
25. Smits R, Hofland N, Edelmann W, et al. Somatic Apc mutations are selected upon their capacity to inactivate the β-catenin down-regulating activity. Genes Chromosomes Cancer 2000;29:229–39.
26. de Wind N, Dekker M, van Rossum A, van der Valk M, te Riele H. Mouse models for hereditary nonpolyposis colorectal cancer. Cancer Res 1998;58:248–55.
27. Edelmann W, Yang K, Kuraguchi M, et al. Tumorigenesis in Mlh1 and Mlh1/Apc1638N mutant mice. Cancer Res 1999;59:1301–7.
28. Prolla TA, Baker SM, Harris AC, et al. Tumour susceptibility and spontaneous mutation in mice deficient in Mlh1, Pms1 and Pms2 DNA mismatch repair. Nat Genet 1998;18:276–9.
29. Chen PC, Dudley S, Hagen W, et al. Contributions by MutL homologues Mlh3 and Pms2 to DNA mismatch repair and tumor suppression in the mouse. Cancer Res 2005;65:8662–70.
30. de Wind N, Dekker M, Claij N, et al. HNPCC-like cancer predisposition in mice through simultaneous loss of Msh3 and Msh6 mismatch-repair protein functions. Nat Genet 1999;23:359–62.
31. Edelmann W, Umar A, Yang K, et al. The DNA mismatch repair genes Msh3 and Msh6 cooperate in intestinal tumor suppression. Cancer Res 2000;60: 803–7.
32. Edelmann W, Yang K, Umar A, et al. Mutation in the mismatch repair gene Msh6 causes cancer susceptibility. Cell 1997;91:467–77.
33. Baker SM, Bronner CE, Zhang L, et al. Male mice defective in the DNA mismatch repair gene PMS2 exhibit abnormal chromosome synapsis in meiosis. Cell 1995;82:309–19.
34. Wienholds E, Plasterk RH. Target-selected gene inactivation in zebrafish. Methods Cell Biol 2004;77: 69–90.
35. Feitsma H, Leal MC, Moens PB, Cuppen E, Schulz RW. Mlh1 deficiency in zebrafish results in male sterility

and aneuploid as well as triploid progeny in females. Genetics 2007;175:1561–9.
36. Desai DC, Lockman JC, Chadwick RB, et al. Recurrent germline mutation in MSH2 arises frequently *de novo*. J Med Genet 2000;37:646–52.
37. Lamberti C, Kruse R, Ruelfs C, et al. Microsatellite instability-a useful diagnostic tool to select patients at high risk for hereditary non-polyposis colorectal cancer: a study in different groups of patients with colorectal cancer. Gut 1999;44:839–43.
38. Stuckless S, Parfrey PS, Woods MO, et al. The phenotypic expression of three MSH2 mutations in large Newfoundland families with Lynch syndrome. Fam Cancer 2007;6:1–12.
39. Moslein G, Tester DJ, Lindor NM, et al. Microsatellite instability and mutation analysis of hMSH2 and hMLH1 in patients with sporadic, familial and hereditary colorectal cancer. Hum Mol Genet 1996;5:1245–52.
40. Yao X, Buermeyer AB, Narayanan L, et al. Different mutator phenotypes in Mlh1- versus Pms2-deficient mice. Proc Natl Acad Sci U S A 1999;96:6850–5.
41. Shimoda N, Knapik EW, Ziniti J, et al. Zebrafish genetic map with 2000 microsatellite markers. Genomics 1999;58:219–32.
42. Berghmans S, Murphey RD, Wienholds E, et al. tp53 mutant zebrafish develop malignant peripheral nerve sheath tumors. Proc Natl Acad Sci U S A 2005;102:407–12.
43. Faucherre A, Taylor GS, Overvoorde J, Dixon JE, Hertog JD. Zebrafish pten genes have overlapping and non-redundant functions in tumorigenesis and embryonic development. Oncogene 2008;27:1079–86.
44. Haramis AP, Hurlstone A, van der Velden Y, et al. Adenomatous polyposis coli-deficient zebrafish are susceptible to digestive tract neoplasia. EMBO Rep 2006;7:444–9.
45. Amsterdam A, Sadler KC, Lai K, et al. Many ribosomal protein genes are cancer genes in zebrafish. PLoS Biol 2004;2:E139.
46. Moore JL, Rush LM, Breneman C, Mohideen MA, Cheng KC. Zebrafish genomic instability mutants and cancer susceptibility. Genetics 2006;174:585–600.
47. Taniguchi Y, Takeda S, Furutani-Seiki M, et al. Generation of medaka gene knockout models by target-selected mutagenesis. Genome Biol 2006;7:R116.
48. Hachem A, Gartenhaus RB. Oncogenes as molecular targets in lymphoma. Blood 2005;106:1911–23.
49. Ehrenstein MR, Neuberger MS. Deficiency in Msh2 affects the efficiency and local sequence specificity of immunoglobulin class-switch recombination: parallels with somatic hypermutation. EMBO J 1999;18:3484–90.
50. Martomo SA, Yang WW, Gearhart PJ. A role for Msh6 but not Msh3 in somatic hypermutation and class switch recombination. J Exp Med 2004;200:61–8.
51. Schrader CE, Vardo J, Stavnezer J. Role for mismatch repair proteins Msh2, Mlh1, and Pms2 in immunoglobulin class switching shown by sequence analysis of recombination junctions. J Exp Med 2002;195:367–73.
52. Schrader CE, Edelmann W, Kucherlapati R, Stavnezer J. Reduced isotype switching in splenic B cells from mice deficient in mismatch repair enzymes. J Exp Med 1999;190:323–30.
53. Danilova N, Bussmann J, Jekosch K, Steiner LA. The immunoglobulin heavy-chain locus in zebrafish: identification and expression of a previously unknown isotype, immunoglobulin Z. Nat Immunol 2005;6:295–302.
54. Feng H, Langenau DM, Madge JA, et al. Heat-shock induction of T-cell lymphoma/leukaemia in conditional Cre/lox-regulated transgenic zebrafish. Br J Haematol 2007;138:169–75.

Zebrafish with Mutations in Mismatch Repair Genes Develop Neurofibromas and Other Tumors

Harma Feitsma, Raoul V. Kuiper, Jeroen Korving, et al.

Cancer Res 2008;68:5059-5066.